⌘ Author's Choice

The Steady-State Repertoire of Human SCF Ubiquitin Ligase Complexes Does Not Require Ongoing Nedd8 Conjugation*[S]

J. Eugene Lee‡, Michael J. Sweredoski§, Robert L. J. Graham§, Natalie J. Kolawa‡, Geoffrey T. Smith§, Sonja Hess§, and Raymond J. Deshaies‡¶‖

The human genome encodes 69 different F-box proteins (FBPs), each of which can potentially assemble with Skp1-Cul1-RING to serve as the substrate specificity subunit of an SCF ubiquitin ligase complex. SCF activity is switched on by conjugation of the ubiquitin-like protein Nedd8 to Cul1. Cycles of Nedd8 conjugation and deconjugation acting in conjunction with the Cul1-sequestering factor Cand1 are thought to control dynamic cycles of SCF assembly and disassembly, which would enable a dynamic equilibrium between the Cul1-RING catalytic core of SCF and the cellular repertoire of FBPs. To test this hypothesis, we determined the cellular composition of SCF complexes and evaluated the impact of Nedd8 conjugation on this steady-state. At least 42 FBPs assembled with Cul1 in HEK 293 cells, and the levels of Cul1-bound FBPs varied by over two orders of magnitude. Unexpectedly, quantitative mass spectrometry revealed that blockade of Nedd8 conjugation led to a modest increase, rather than a decrease, in the overall level of most SCF complexes. We suggest that multiple mechanisms including FBP dissociation and turnover cooperate to maintain the cellular pool of SCF ubiquitin ligases. ***Molecular & Cellular Proteomics 10: 10.1074/mcp.M110.006460, 1–9, 2011.***

Proteins in the cell are in a dynamic state—they are continuously being synthesized and degraded to maintain intracellular protein homeostasis. The majority of intracellular protein degradation is controlled by the ubiquitin-proteasome system. Ubiquitin-proteasome system-mediated protein degradation comprises two major successive steps (1, 2). The first step is the covalent assembly of a chain of the small protein ubiquitin on target proteins. This first step is catalyzed by the sequential action of three different classes of enzymes. Ubiquitin-activating enzyme (E1) catalyzes the activation of ubiquitin, which is subsequently transferred to ubiquitin-conjugating enzyme (E2). E2 charged with ubiquitin collaborates with ubiquitin ligase (E3) to ubiquitylate the target substrate. Multiple ubiquitin transfers may occur in a successive manner, resulting in the processive formation of an ubiquitin chain (3). The second step is the energy-dependent proteolysis of the ubiquitin chain-tagged protein by the 26S proteasome complex.

There are nearly 600 ubiquitin ligases encoded in the human genome, and up to 241 (over 40%) are potentially drawn from the cullin–ring ligase (CRL)[1] family (K. Hofmann, personal communication). The biological significance of CRLs is manifested by the fact that about 20% of the proteasome-dependent cellular protein degradation is dependent on CRL activity (4). CRLs are modular multisubunit complexes composed of a cullin subunit that serves as an organizing scaffold, an E2-recruiting RING subunit, an adaptor protein, and a substrate recognition subunit (5). In the SCF complex (*S*kp1 adaptor; *C*ul1 scaffold; *F*-box substrate recognition subunit), the prototypical CRL, common subunits are shared except for the F-box protein (FBP) that recruits substrate. Thus, the enzymatic identity of an SCF complex is designated by its FBP subunit. Up to 69 loci that encode FBPs are found in the human genome, alluding to the possibility of the same number of different SCF complexes (6). It is a matter of debate, however, whether all 69 FBPs can assemble into an SCF complex. For example, the yeast FBPs Ctf13 and Rcy1 do not form stable complexes with Cul1 (7, 8). Of the 69 possible SCF complexes, several have been identified and investigated in great detail, but the vast majority remains to be explored.

A second unresolved question about the network of SCF ubiquitin ligases is, how is the assembly of 69 different SCF complexes regulated? We and others (9–11) have proposed that the Cul1-RING (the SCF RING subunit is known as either Rbx1, Roc1, or Hrt1) catalytic core of SCF cycles dynamically between an assembled, active state and a disassembled, inactive state (hereafter referred to as the "Cul1 cycle") (Fig. 1). The active state is represented by Cul1 bound to FBP-Skp1 and conjugated with the ubiquitin-like modifier Nedd8 at

From the ‡Division of Biology, §Proteome Exploration Laboratory, Beckman Institute, and ¶Howard Hughes Medical Institute, California Institute of Technology, Pasadena, CA 91125

Received November 16, 2010, and in revised form, December 13, 2010
⌘ *Author's Choice*—Final version full access.
Published, MCP Papers in Press, December 17, 2010, DOI 10.1074/mcp.M110.006460

[1] The abbreviations used are: CRL, cullin—ring ligase; FBP, F-box protein; CSN, COP9 signalosome; SILAC, stable isotope labeling with amino acid in cell culture.

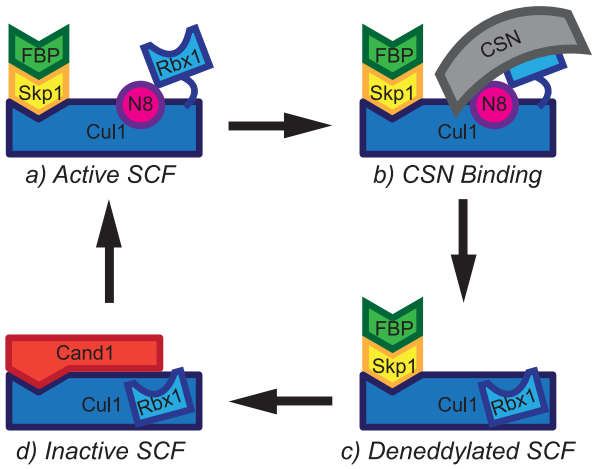

FIG. 1. **The Cul1 Cycle**. *A*, Cul1 complexed with FBP-Skp1 and covalently modified with Nedd8 (N8) represents an active SCF. *B* and *C*, Inactivation of SCF initiates when CSN binds active SCF and deconjugates Nedd8, returning the RING subunit Rbx1 to its inactive configuration. *D*, Cand1 dislocates FBP-Skp1 and binds Cul1, forming an inactive Cand1-Cul1 complex. Restoration of an active SCF complex is brought upon by the combined action of Nedd8-conjugating enzymes and FBP-Skp1. Conjugation of Nedd8 causes a major conformational change in Cul1 and E2-recruiting Rbx1. This dynamic cycle of Cul1 is thought to enable a rapid sampling of the steady-state FBP-Skp1 population.

Lys720. This modification (neddylation) causes a major conformational change in the cullin and RING subunits (12), and increases ubiquitin ligase activity (12–14). Inactivation of SCF is initiated by deconjugation of Nedd8 (deneddylation) by the COP9 signalosome complex (CSN) (15), which houses a metallo-isopeptidase subunit (9). Once deneddylated, Cul1 becomes available to the sequestration factor Cand1, which dislocates FBP-Skp1 to establish an enzymatically inactive Cand1-Cul1 complex (16, 17). Because Cand1 partially occludes both the FBP-Skp1 binding site and Lys720 on Cul1, the active and inactive states of Cul1 are mutually exclusive. The Cul1 cycle is completed by the dissolution of the Cand1-Cul1 complex by the combined action of Nedd8-conjugating enzymes and FBP-Skp1, resulting in the reformation of an intact, Nedd8-conjugated SCF complex (18, 19). It has been suggested that dynamic cycles of assembly/disassembly remodel the repertoire of SCF complexes in accordance with cellular requirements (9, 11). Although this hypothesis is attractive, many of its predictions remain to be tested. Specifically, it remains unclear whether SCF complexes undergo cycles of assembly/disassembly in cells, and to what extent such cycles are driven by Nedd8 conjugation and deconjugation.

Here, we probe the Cul1 network and the proposed Cul1 cycle using mass spectrometry. First, we determined the repertoire of SCF complexes in HEK 293 cells. We found at least 42 FBPs assembled with Cul1 in HEK 293 cells, with abundance of the complexes varying over two orders of magnitude. Second, we tested a key prediction of the current model for how SCF complexes dynamically assemble and disassemble by evaluating the composition of SCF complexes in cells in which Nedd8 conjugation was blocked by the inhibitor MLN4924 (4). According to the current model, loss of Cul1 neddylation is predicted to bring about a shift in the SCF equilibrium in favor of disassembly. Using the quantitative stable isotope labeling with amino acid in cell culture (SILAC) approach, we show that MLN4924 actually increased FBP-Skp1 association with Cul1.

EXPERIMENTAL PROCEDURES

Chemicals and Reagents—MagneHis Ni-Particles and sequencing grade trypsin were purchased from Promega. High Capacity Neutravidin Agarose Resin, n-dodecyl-β-D-maltoside, and SuperSignal West Dura Extended Duration chemiluminescent substrate were obtained from Thermo Scientific. Lysyl endopeptidase (LysC) was obtained from Wako Chemicals (Richmond, Va). Cell culture reagents, Flip-In T-REx 293 cells, plasmids, and monoclonal antibodies for Cul1 and Cand1 were obtained from Invitrogen. Plasmid DNA containing the human Cul1 sequence was purchased from Open Biosystems. MLN4924 was a generous gift from Millennium: The Takeda Oncology Company. All other general chemicals for buffers were purchased from Fisher Scientific and/or VWR International.

Plasmid and Cloning—The HTBH tag (20) was a generous gift from the Kaiser group. This tag contains a TEV cleavage site, two hexa-His sequences, and a biotinylation signal sequence. Biotinylation is catalyzed by endogenous biotin ligases, which are present in all eukaryotic cells (21). The HTBH tag was appended to the C terminus of the human Cul1 and sequences encoding Cul1^{HTBH} were inserted into the pCDNA5/FRT/TO plasmid.

Construction of Stable Cell Line—Flip-In T-REx 293 cells contain a single stably integrated FRT site at a transcriptionally active genomic locus. For targeted integration of CUL1^{HTBH} into the FRT site, co-transfection of Cul1^{HTBH}/pCNDA5/FRT/TO vector and Flp recombinase vector pOG44 was performed using Lipofectamine 2000 (Invitrogen). One day after transfection, 100 μg/ml hygromycin was added to the medium to select for the cells with intergrated sequences coding for Cul1^{HTBH}. It took 2 weeks for visible colonies to appear. Five colonies were picked and expanded to confirm tetracycline-dependent expression of Cul1^{HTBH}. Expanded colonies were grown in medium containing 10% fetal bovine serum, 1% penicillin/streptomycin, and 50 μg/ml hygromycin. For SILAC, Dulbecco's modified Eagles medium (DMEM) lacking arginine and lysine was used, along with 10% dialyzed fetal bovine serum. For heavy labeling, Arg6 (U-^{13}C6) and Lys8 (U-^{13}C6, U-^{15}N2) (Cambridge Isotopes, Andover, MA) were supplemented at the same concentration as in the standard DMEM formulation. For light labeling, regular DMEM was used. Following 10 passages in heavy medium, label incorporation rates were measured by acid hydrolysis of lysates as described previously (22).

Two-step Purification of Cul1^{HTBH}—To induce the expression of HTBH-tagged Cul1 in cells at 50% confluency, 1.0 μg/ml tetracycline was added to the medium for 4 h. This expression condition ensured that the level of tagged Cul1 was similar to that of endogenous Cul1. Following induction, cells were allowed to grow for 24 h. Deneddylation of Cul1 was effected by treating Cul1-induced cells with 100 nM MLN4924 for 24 h. Cells were trypsinized and washed two times with ice-cold phosphate buffered saline buffer. The cell pellets were collected and lysed in lysis buffer (50 mM HEPES, pH 7.5; 70 mM KOAc; 5 mM $Mg(OAc)_2$; 20 mM imidazole, 0.2% n-dodecyl-β-D-maltoside) containing 1× protease inhibitor (Roche) for 30 min on a gyrating platform at 4 °C. The lysates were centrifuged at 16,600 × *g* for 15

min to remove cell debris, and the supernatant was incubated with MagneHis Ni particles (30 μl particles/mg lysate) on a gyrating platform for 90 min at 4 °C. The MagneHis particles were then washed with 20 bed volumes of the lysis buffer three times, followed by a 10-min elution with 10 bed volumes of elution buffer (50 mM HEPES, pH 7.5; 70 mM KOAc; 5 mM $Mg(OAc)_2$; 300 mM imidazole, 0.2% n-dodecyl-β-D-maltoside). Eluant was incubated with Neutravidin beads (10 μl beads/mg lysate) on a gyrating platform for 90 min at 4 °C. Neutravidin beads were washed with lysis buffer three times and then washed with 100 mM Tris-HCl (pH 8.5) two times.

Mass Spectrometric Analysis—At the last step of the tandem affinity purification, the proteins were bound on Neutravidin beads for a direct on-bead digestion. Digestion was performed in 100 mM Tris-HCl (pH 8.5) containing 8 M urea at 37 °C first with Lys-C (35 ng/mg lysate) for 4 h, and then the urea concentration was reduced to 2 M for trypsin (30 ng/mg lysate) digestion overnight. Following digestion, the tryptic peptides were desalted on a reversed-phase Vivapure C18 micro spin column (Sartorius Stedim Biotech, Gottingen, Germany), and concentrated using a SpeedVac. Dried samples were acidified by 0.2% formic acid prior to mass spectrometric analysis. All liquid chromatography-mass spectrometry experiments were performed on an EASY-nLC (Proxeon Biosystems, Waltham, MA) connected to a hybrid LTQ-Orbitrap Classic (Thermo Scientific) equipped with a nano-electrospray ion source (Proxeon Biosystems) essentially as previously described (23) with some modifications. Peptides were separated on a 15 cm reversed phase analytical column (75 μm internal diameter) packed in-house with 3 μm C18AQ beads (ReproSil-Pur C_{18AQ}) using a 160-min gradient from 12% to 30% acetonitrile in 0.2% formic acid at a flow rate of 350 nL/minute. The mass spectrometer was operated in data-dependent mode to automatically switch between full-scan MS and tandem MS acquisition. Survey full scan mass spectra were acquired in Orbitrap (300–1700 *m/z*), following accumulation of 500,000 ions, with a resolution of 60,000 at 400 *m/z*. The top ten most intense ions from the survey scan were isolated and, after the accumulation of 5000 ions, fragmented in the linear ion trap by collisionally induced dissociation (collisional energy 35% and isolation width 2 Da). Precursor ion charge state screening was enabled and all singly charged and unassigned charge states were rejected. The dynamic exclusion list was set with a maximum retention time of 90 s, a relative mass window of 10 ppm and early expiration was enabled. The raw data can be downloaded from Tranche at https://proteomecommons.org/dataset.jsp?i=CE7O4IntpkSJ7mnej1%252FTWma0CVpb4rjb1XFl2LjQ%252BV4cnzlMGTVnj%25

Data Analysis—Peak lists were generated from raw data files using MaxQuant (version 1.0.13.13) (24). Peak lists were then submitted to the database search engine Mascot (version 2.2.06; www.matrixscience.com) and searched against the IPI human database (v 3.54) and a contaminant database concatenated to a decoy database prepared as described in (24). There were 75,668 target database sequences with 262 contaminant sequences, and an equal number of decoy sequences. The search parameters were tryptic digestion, maximum of two missed cleavages, fixed carboxyamidomethyl modifications of cysteine, variable oxidation modifications of methionine, and variable protein N-terminal carbamylations. Mass tolerance for precursor ions were 7 ppm and that for fragment ions were 0.5 Da. Protein inference and quantitation were performed by MaxQuant with 1% false discovery rate thresholds for both peptides and proteins. Using our stringent setting, at least two different peptide sequences were required for protein identification and two different ratio measurements were required for protein quantitation. When single peptide identifications were also accepted, two additional FBPs (Fbxo20 and Fbxl6) were identified and quantified. Peptide intensities from the unique peptides were used for quantitation. To estimate the reliability of the fold changes for the SILAC data, the total number of independent ratio measurement is given as well as the 95% confidence interval of the median of all measurements, which was calculated by bootstrap estimation. For emPAI value calculation, modified and shared peptides were included for counting.

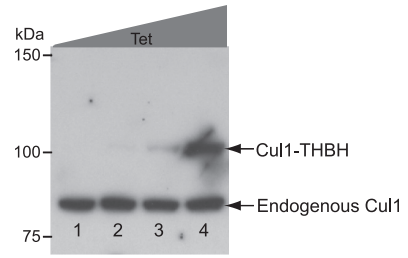

FIG. 2. **Generation of a stable cell line expressing tagged Cul1 upon tetracycline treatment.** Flip-In T-REx 293 cells were transfected with pCDNA5/FRT/TO vector containing sequences encoding $Cul1^{HTBH}$, and selected with hygromycin (100 μg/ml). Selected cells were induced with the indicated amount of tetracycline for 4 h (Lane 1, no tetracycline; Lane 2, 0.2 μg/ml, Lane 3, 0.5 μg/ml; Lane 4, 1.0 μg/ml). After induction, cells were grown for 24 h and lysed for Western blot analysis.

RESULTS

Generation of Stable Cell Line Expressing Tagged Cul1—To create a system that would facilitate the purification of Cul1 and its interacting proteins, we constructed a stable cell line that expressed HTBH-tagged Cul1 ($Cul1^{HTBH}$) upon tetracycline treatment. Flip-In T-Rex 293 cells cotransfected with the pCDNA5/FRT/TO vector containing sequences encoding $Cul1^{HTBH}$ and the pOG44 plasmid encoding recombinase yielded visible colonies in 2 weeks under selective medium (100 μg/ml hygromycin). Individual colonies were tested for the level of $Cul1^{HTBH}$ expression (Fig. 2). Western blot analysis confirmed that tagged Cul1 was expressed at the same level as the endogenous protein, which should diminish any non-physiological protein-protein interactions that may be caused by overexpression. The induction condition described (1.0 μg/ml tetracycline, 4 h) was used for all of the experiments involving the expression of $Cul1^{HTBH}$.

Analyses of Cul1 Proteome—To reveal the Cul1 proteome, we carried out liquid chromatography (LC)-tandem MS (MS/MS) (LTQ-Orbitrap) analyses of the Cul1-associated proteins following tandem affinity purification of $Cul1^{HTBH}$. To gain a comprehensive picture, we analyzed 22 biological replicates, because we reasoned that the peptides from low abundance proteins might fall below the range of detection in any single analysis. As expected, some FBPs were found only in a few experiments (supplemental Table S1), confirming the validity of our approach. Overall, we detected 42 different FBPs, Skp1, Rbx1/Roc1/Hrt1, all the subunits for CSN, Cand1 and Cand2, and 4 Dcn1-like proteins (Table I). This list comprises the largest recorded Cul1 proteome to date. Strikingly, no ubiquitin-conjugating enzymes (E2) were detected.

A recent report suggested that the proline residue in the conserved LP motif of the F-box is important for distinguishing between FBPs that associate with Cul1 from those that do

TABLE I
Summary of proteins associated with Cul1

Proteins[a]	Spectral counts[b]	Number of observable peptides[c]	Number of observed peptides	emPAI[d]
Cul1	15815	631	117	0.53
Cand1	11218	303	131	1.7
Cand2	372	271	34	0.33
Skp1	1725	43	21	2.08
Rbx1	736	18	11	3.08
Dcn1-like				
Dcund1	183	90	15	0.47
Dcund2	4	92	3	0.078
Dcund4	56	117	8	0.17
Dcund5	179	81	20	0.77
Signalosome				
Csn1	651	168	27	0.39
Csn2	800	153	38	0.77
Csn3	698	85	31	1.31
Csn4	969	134	35	0.82
Csn5	604	79	29	1.33
Csn6	557	66	21	1.08
Csn7a	241	92	17	0.53
Csn7b	276	80	15	0.54
Csn8	340	30	11	1.33
F-box				
Fbxl18	788	167	43	0.90
Fbxo7	653	117	25	0.64
Skp2 (Fbxl1)	646	85	26	1.02
Fbxo21	532	122	30	0.76
Fbxo9	393	153	29	0.55
Fbxo18	173	334	27	0.20
Fbxo42	299	118	25	0.63
Fbxo22	310	102	23	0.68
Fbxw11	232	179	25	0.38
Fbxo44[e]	278	83	12	0.40
Fbxo17	259	93	17	0.52
Fbxl15	227	121	20	0.46
Fbxo3	226	119	24	0.59
Fbxw1a	133	213	14	0.16
Fbxo38	12	328	5	0.036
Fbxo11	152	174	20	0.30
Fbxo10	10	278	3	0.025
Fbxo30	152	132	21	0.44
Fbxo44[f]	194	63	12	0.55
Fbxo46	54	190	10	0.13
Fbxo4	159	75	13	0.39
Fbxl12	120	100	14	0.38
Fbxw9	100	115	17	0.41
Fbxl14	76	123	11	0.29
Fbxo5	19	175	7	0.096
Fbxw8	64	123	12	0.25
Fbxo31	27	154	10	0.16
Fbxo33	37	142	6	0.10
Fbxw4	7	172	2	0.027
Fbxw5	31	130	7	0.13
Fbxl20	26	129	8	0.15
Fbxo28	13	139	4	0.069
Fbxl17	6	142	2	0.033
Fbxo6	65	81	7	0.22
Fbxl6	6	139	1	0.017
Fbxl8	45	99	8	0.20
Fbxo25	3	130	2	0.036
Fbxw2	14	110	6	0.13
Fbxl4	13	106	11	0.23
Fbxo8	31	84	9	0.28
Fbxo20	2	642	1	0.0036
Fbxo45	13	76	4	0.13

[a] Total spectral counts in 22 biological replicates.
[b] Proteins are filtered at a 1% false discovery rate.
[c] Observable peptides are defined as tryptic peptides with mass between 600 and 4500 Da calculated by an in-house script, allowing up to three mis-cleavages from the first leading protein sequence.
[d] emPAI = $10^{(\#\text{ of observed peptides}/\#\text{ of observable peptides})} - 1$.
[e] International Protein Index IPI00013239.
[f] International Protein Index IPI00414844.

not (10). Nevertheless, the FBPs we identified in Cul1^{HTBH} immuno-precipitates included ones that lack this proline residue (*e.g.* Fbxl18 and Fbxl14; alignment based on the Pfam database model (25)) (supplemental Table S2). Extensive bioinformatic searches failed to identify a characteristic motif that distinguished FBPs found in Cul^{HTBH} immuno-precipitates from those not found. It is possible that most of the undetected FBPs were not expressed in HEK 293 cells or were expressed at a level that was too low to detect. A summary of all human F-boxes is described in supplemental Table S2.

To estimate the abundance of individual Cul1-associated proteins, we adopted emPAI (Exponentially Modified Protein Abundance Index). This index offers approximate, label-free, relative quantification of proteins based on peptide recovery (26). The emPAI value for the detected FBPs ranged from 0.0036 to 1.02, with Skp2 scoring the highest number. Whereas some highly abundant FBPs have been popular subjects of study as indicated by their frequency of appearance in PUBMED keyword searches (*e.g.* Skp2, 625 publications; Fbxw1a, 303 publications), it is interesting to note that many of the most abundant FBPs await future characterization (Fig. 3).

Among shared Cul1 interactors, Rbx1 had the highest emPAI value of 3.08, followed by Skp1 (2.08) and Cand1 (1.7). The high emPAI value of Rbx1 is consistent with it being a stoichiometric binding partner of Cul1 (16, 27). We found every subunit of CSN with emPAI values (0.39–1.33) comparable to those of abundant FBPs. This finding, whereas consistent with immuno-precipitation data, is unusual considering that the nature of CSN-Cul1 association is that of enzyme-substrate/product interaction, which in general is transient.

Deneddylation Does not Have a Major Effect on Cul1 Proteome—The current model for SCF regulation posits that Cul1 constantly cycles between states in which it is bound to either the sequestration factor Cand1 or to FBP-Skp1 complexes (9, 10). This cycle is thought to be fueled by the enzymes that

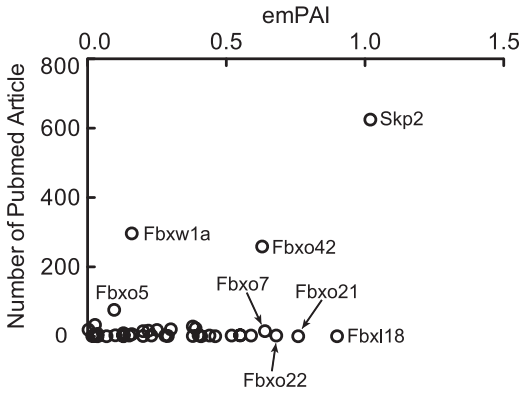

FIG. 3. **Correlation of the emPAI values and number of Pubmed articles for F-box proteins.** Representative F-box proteins that are either intensively studied or found at high levels in Cul1 immunopreciptates are labeled.

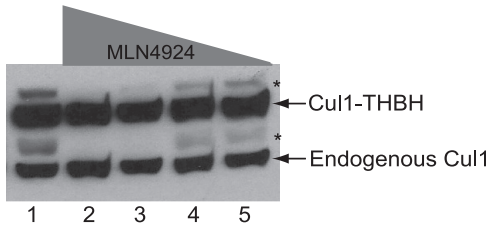

FIG. 4. **Effect of MLN4924 on the neddylation status of Cul1.** Flip-In T-REx 293 cells with an integrated *CUL1-HTBH* gene (Fig. 2) were induced with 1.0 μg/ml tetracycline for 8 h. Cells were grown 24 h before being treated with the indicated amount of MLN4924 for an additional 24 h (Lane 1, no MLN4924; Lane 2, 100 nM; Lane3, 50 nM, Lane 4, 10 nM, Lane 5, 5 nM). Cells were lysed with lysis buffer containing 1 mM 1,10-phenanthroline, a zinc chelator that blocks the deneddylating activity of the COP9 signalosome (CSN). Neddylated species for both Cul1^{HTBH} and the endogenous Cul1 are indicated with the asterisk marks.

promote conjugation and deconjugation of Nedd8. Conjugation of Nedd8 to Lys720 of Cul1 promotes dissociation of the Cand1-Cul1 complex and thereby facilitates incorporation of Cul1 into an active SCF complex, whereas deconjugation of Nedd8 by CSN enables resequestration of Cul1 into a complex with Cand1. According to this model, blockade of Nedd8 conjugation should lead to rapid depletion of SCF complexes as Cul1 becomes deneddylated by CSN and captured by Cand1. To assess the dynamic behavior of the Cul1 cycle, we sought to perturb Cul1 neddylation with MLN4924. MLN4249 exerts its deneddylating activity by forming a covalent, irreversible adduct with Nedd8 (28). The Nedd8-MLN4924 adduct binds tightly to NAE, blocking the action of this enzyme. Strikingly, upon treatment with MLN4924 nearly all neddylated Cul1 is depleted within 5 min (4); this result indicates that Cul1 is subject to continuous, rapid deneddylation by CSN, implying that the Cul1 cycle runs constitutively at a rapid rate. The properties of MLN4924 suggested that it would be an ideal agent to test the current model for SCF dynamics, and so we sought to evaluate the effect of MLN4924 on the Cul1 proteome using SILAC (stable isotope labeling with amino acid in cell culture)-based quantitative mass spectrometry.

We first confirmed the impact of MLN4924 on Cul1^{HTBH} neddylation. Fig. 4 shows that 100 nM MLN4924 drove near complete elimination of Nedd8 from both endogenous Cul1 and Cul1^{HTBH}. We next carried out SILAC experiments, wherein parallel cultures of HEK 293 cells expressing Cul1^{HTBH} were grown, with one culture labeled with light amino acids and the other labeled with heavy arginine and lysine (Arg6 and Lys8). These cultures were either mock-treated or supplemented with 100 nM MLN4924 for 24 h, following which the cells were mixed, lysed and Cul1^{HTBH} complexes were retrieved by immuno-precipitation and analyzed by mass spectrometry. Table II summarizes the results from 10 independent analyses. Our original expectation was that the net deneddylation caused by MLN4924 treatment would have reciprocal effects on Cand1 and FBP-Skp1 association with Cul1, with Cand1 association increasing and FBP-Skp1 association decreasing. On the contrary, the amount of Cand1 bound to Cul1 slightly decreased in MLN4924-treated cells, whereas the amount of Skp1 (up by 1.19-fold) and FBPs (up by 1.30-fold on average) slightly increased. Similar results were obtained when shorter MLN4924 treatments were applied (4 and 8 h, data not shown), and regardless of whether the MLN4924-treated culture was encoded with light or heavy amino acids. These results are opposite to what the current model predicts, and indicate that Nedd8 deconjugation does not lead to the net loss of SCF complexes.

Free Cand1 is Not Limiting in MLN4924-treated cells—One potential problem with the approach described above is that it did not exclude the possibility that the inhibition of neddylation triggered the complete arrest of the Cul1 cycle. For example, consider the possibility that the molecule of Cand1 that promotes disassembly of one SCF complex is liberated by assembly of another SCF complex—that all of the Cand1 in a cell is bound to cullins, and disassembly of SCF complexes requires the continuous liberation of Cand1 by ongoing neddylation. In this view, shutting off Nedd8 conjugation would be equivalent to shutting off the spigot that supplies Cand1, thereby "freezing" the Cul1 cycle. In this case, one would not observe the expected effect of deneddylation (*i.e.* increased Cand1 and decreased Skp1 and FBPs bound to Cul1), if there is little pre-existing free Cand1. To test this possibility, we designed a simple reversed order-of-addition experiment. Unlike the SILAC experiments, the MLN4924 treatment was initiated prior to the induction of Cul1^{HTBH} synthesis by tetracycline. Newly synthesized Cul1^{HTBH} was affinity-purified and the amount of Cand1 retrieved was compared with a mock-treated sample. If free Cand1 becomes limiting in MLN4924-treated cells because of stoppage of the Cul1 cycle, Cul1^{HTBH} synthesized following MLN4924 treatment would not have access to Cand1; therefore, the level of Cand1 associated with newly-synthesized Cul1^{HTBH} should be much less in

TABLE II
Quantitative analysis of proteins associated with Cul1 upon inhibition of neddylation

Proteins[a]	Fold change[b,c]	Number of ratio measurements[d]
Cul1	1.00 (0.99–1.01)	4154
Cand1	0.92 (0.91–0.93)	2584
Skp1	1.19 (1.16–1.21)	476
Rbx1	1.00 (0.97–1.02)	183
Dcn1-like		
Dcund1	0.85 (0.82–0.91)	22
Dcund2	0.95 (0.80–1.07)	6
Dcund4	0.93 (0.85–1.02)	14
Dcund5	0.94 (0.88–0.98)	172
Signalosome		
Csn1	0.98 (0.96–1.00)	472
Csn2	1.01 (0.93–1.13)	13
Csn3	0.98 (0.96–1.00)	460
Csn4	0.96 (0.94–0.98)	648
Csn5	0.95 (0.94–0.98)	348
Csn6	0.99 (0.98–1.02)	315
Csn7a	0.91 (0.87–0.94)	182
Csn7b	1.02 (0.98–1.07)	158
Csn8	1.01 (0.97–1.04)	156
F-box		
Fbxo18	2.06 (2.01–2.20)	155
Fbxw5	2.04 (1.86–2.24)	16
Fbxl6	2.04 (1.59–2.49)	7
Fbxl17	1.91 (1.20–3.24)	6
Fbxo46	1.90 (1.36–2.99)	16
Fbxo31	1.79 (1.71–2.06)	25
Fbxw1a	1.60 (1.49–1.74)	40
Fbxo21	1.52 (1.45–1.57)	234
Fbxo38	1.51 (1.24–1.67)	13
Fbxo33	1.50 (1.40–1.62)	47
Fbxo22	1.50 (1.43–1.55)	139
Fbxo28	1.49 (1.29–1.59)	11
Fbxo17	1.48 (1.38–1.54)	40
Skp2 (Fbxl1)	1.42 (1.39–1.49)	201
Fbxw2	1.42 (1.29–1.62)	10
Fbxw9	1.31 (1.27–1.47)	61
Fbxo44[e]	1.30 (1.22–1.46)	37
Fbxl20	1.29 (1.20–1.31)	3
Fbxw11	1.28 (1.25–1.34)	89
Fbxo5	1.24 (1.12–1.38)	10
Fbxo30	1.23 (1.17–1.28)	114
Fbxo7	1.21 (1.16–1.28)	244
Fbxl12	1.20 (1.15–1.25)	95
Fbxo42	1.19 (1.12–1.25)	123
Fbxo3	1.14 (1.10–1.18)	107
Fbxo6	1.13 (0.98–1.30)	7
Fbxo44[f]	1.11 (1.05–1.20)	28
Fbxl14	1.09 (1.05–1.14)	36
Fbxo10	1.07 (0.85–1.09)	11
Fbxl18	1.05 (1.02–1.08)	258
Fbxo4	1.03 (0.97–1.12)	44
Fbxl8	1.03 (0.93–1.08)	29
Fbxw8	1.01 (0.98–1.06)	47
Fbxl15	1.01 (0.96–1.17)	91
Fbxo45	0.97 (0.27—1.05)	7
Fbxo8	0.96 (0.90–1.23)	17
Fbxo9	0.93 (0.91–0.97)	206
Fbxw4	0.92 (0.78–0.95)	4
Fbxo11	0.67 (0.61–0.87)	83
Fbxl3	0.31 (0.26–2.03)	5
Average F-box	1.30	

[a] Proteins are filtered at a 1% false discovery rate.
[b] Median values for H/L from the SILAC experiments where heavy cells are treated with 100 nM MLN4924 for 24 hours. When light cells were treated with MLN4924, H/L was reversed. Values were normalized so that H/L for Cul1 was 1.
[c] 95% confidence interval calculated by bootstrap estimation is shown in the parentheses.
[d] Peptides from ten biological replicates were used for quantitation by the program MaxQuant.
[e] International Protein Index IPI00647771.
[f] International Protein Index IPI00414844.

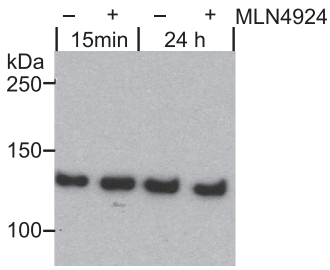

FIG. 5. **Effect of MLN4924 on the availability of free Cand1.** Flip-In T-REx 293 cells with an integrated *CUL1-HTBH* gene were mock-treated or treated with MLN4924 (3 μM MLN4924 for 15 min treatment and 100 nM MLN4924 for 24 h treatment) prior to tetracycline induction. Following this first treatment period, $Cul1^{HTBH}$ was expressed with 2 μg/ml tetracycline for 2 h, keeping MLN4924 present in the MLN4924-treated samples. Following cell lysis, newly synthesized $Cul1^{HTBH}$ was affinity purified, and the amount of Cul1-bound Cand1 was analyzed by Western blot.

MLN4924-treated cells compared with cells that were not exposed to MLN4924. Yet, Western blot analyses showed that the amount of Cand1 associated with $Cul1^{HTBH}$ was almost identical regardless of whether the $Cul1^{HTBH}$ was synthesized in cells exposed to MLN4924 for either 15 min. or 24h, or mock-treated (Fig. 5). This result is consistent with absolute quantification of the free and bound pools of Cand1 (J.W. Harper, personal communication) and confirms that there is enough free Cand1 available for complex formation with Cul1 even after the complete loss of Nedd8 conjugation.

DISCUSSION

CRLs represent approximately one third of human ubiquitin ligases. Despite a strong emerging consensus that CRLs play key roles in diverse aspects of human biology, several fundamental questions remain unanswered including, how are the assembly and cellular repertoire of these modular, multisubunit ligases dynamically regulated? To address these issues, we took a quantitative proteomic approach with Cul1, which serves as the organizing scaffold of SCF, the prototype for the CRL family. We first obtained a static representation of the

Cul1 proteome, surveying how many different SCF complexes can be detected in a single cell type. Using a HEK 293-derived cell line that expresses a tandem-tagged Cul1 at levels similar to the endogenous protein, we determined that Cul1 interacted with at least 42 different FBPs. Thus, at least 60% of the FBPs encoded in the human genome can form SCF complexes with Skp1-Cul1-Rbx1. We did not detect five FBPs that are known to interact with Cul1 (Fbxo1, Fbxo2, Fbxo32, Fbxl5, and Fbxw7), presumably because of their low (or lack of) expression in HEK 293 cells; thus, 47 represents the minimum estimate of the number of different SCF complexes that can form in human cells.

In addition to FBPs, our proteomic analysis detected the known shared core subunits including Rbx1 and Skp1, as well as the regulatory factors Cand1 and 2, Dcund1, 2, 4, and 5, and CSN. It is worthwhile to mention that we did not detect any E2 enzymes in our analyses. Identifying the physiological E2 partner for an E3 ubiquitin ligase is of great importance, because E2 enzymes are thought to determine the nature of the ubiquitin chain attached to the target substrate, which determines the subsequent cellular fate of the conjugate. Failure to detect an E2 enzyme is consistent with the observation that SCF-Cdc34 (Cdc34 is an E2 for SCF) interactions are extremely transient (29), and thus were presumably lost during the affinity purification step. In this regard, we still lack a reliable methodology for determining the complete functionally-relevant proteome for SCF ubiquitin ligases by mass spectrometry.

Among identified binders of Cul1, FBPs are of special interest because these proteins render substrate specificity to the SCF complex. FBPs are classified into three major subcategories—FBXLs, FBXWs, and FBXOs—based on the type of substrate interaction domain linked to the F-box (6). As shown in Table I, we found all three F-box subclasses in association with Cul1. Based on a recent report that a critical proline residue within the F-box determines whether a given FBP assembles with Cul1 (10), we performed extensive bioinformatic analyses focusing on the 40-amino acid F-box. Our data do not reveal a motif that distinguishes FBPs that were detected Cul1 immuno-precipitates from those that were not and are in conflict with the prior report, because three of the FBPs detected in our experiments lack the critical proline (supplemental Table S2). It is possible, however, that these proline-less FBPs interact indirectly as a substrate or dimerize with proline-containing FBPs (30, 31).

Our data indicate that HEK 293 cells assemble at least 42 different SCF complexes, each defined by its characteristic FBP subunit. Skp1-Cul1-Rbx1 is not shared equally by the different FBPs, in that FBP abundance (estimated based on emPAI values) varied by two orders of magnitude. Future work will reveal whether this variation is driven by differences in expression level *versus* differences in assembly. It seems likely that some less abundant SCF complexes were left unidentified because of limits to the sensitivity of the methodology used in this study, so the difference in abundance could be even more significant. A close assessment of the emPAI values for the identified FBPs shed light on another interesting aspect of our findings. With Skp2 exhibiting the highest emPAI value of 1.02, SCF^{Skp2} could be considered to be one of the most abundant SCF complexes in HEK 293 cells. Skp2 is also the most intensively studied FBP. A search of the PUBMED database with the keywords skp2, fbl1, or fbxl1 yielded 625 papers, which is the greatest number among all F-box proteins (Fig. 3). Skp2 was one of the first human FBPs to be discovered (32), which was enabled by its relative abundance. It is therefore most intriguing to consider that of the ten FBPs on our list with the highest emPAI values, eight are poorly (or not at all) characterized. For example, Fbxl18 and Fbxo21, the FBPs with the highest emPAI values and the highest total spectral counts, have zero references in the PUBMED database. The combined reference count for these eight poorly studied F-box proteins is only 27. This simple fact highlights that there is a great amount that remains to be learned about the biology of SCF complexes.

Given the large number of distinct FBP-Skp1 complexes in human cells that compete for a common Cul1-Rbx1 catalytic core, a key question is, how is the cellular repertoire of SCF complexes controlled? Several lines of evidence suggest that SCF complexes undergo constant cycles of assembly and disassembly, and this allows the Cul1-Rbx1 catalytic core to continuously and rapidly sample the steady-state population of FBP-Skp1 complexes. It has been proposed that cycling of SCF complexes is driven by Nedd8 conjugation and deconjugation enzymes working in concert with the sequestration factor Cand1. Deneddylation of the entire population of cullin proteins occurs at a very fast rate, as indicated by rapid loss of Nedd8 conjugates upon inhibition of NAE (4). Once it is deneddylated, Cul1 can bind to the sequestration factor Cand1, which displaces FBP-Skp1 (16, 17, 33). A core prediction of this hypothesis is that in cells in which Nedd8 conjugation is abruptly halted, Cand1 should displace FBP-Skp1 from deneddylated Cul1, and there should be net loss of SCF complexes. By contrast, in quantitative mass spectrometry experiments, we detected less Cand1 and more FBP-Skp1 bound to Cul1 after incubation with the Nedd8 conjugation inhibitor MLN4924. We have shown that this is not because of depletion of free Cand1 in MLN4924-treated cells (Fig. 5). It is also unlikely that the nature or position of the epitope tag is responsible for the persistence of SCF complexes in MLN4924-treated cells because a similar result was observed with a FLAG-HA tag appended to the N terminus of cullins (J.W. Harper, personal communication). Notably, the steady-state level of Nedd8-conjugated Cul1 was much higher in the cell line employed by Harper and colleagues (~50% in HEK 293T *versus* 5–10% in our HEK 293 cells), suggesting that the initial steady-state neddylation does not determine the response to MLN4924.

There are three possible explanations for this unexpected effect of MLN4924 treatment on the Cul1 proteome: (i) synthesis of most FBPs is slightly up-regulated upon MLN4924 treatment, (ii) MLN4924 shifts the equilibrium between free Cul1-Rbx1 and FBP-Skp1 in favor of assembly, so there are more SCF complexes even though the total level of FBPs does not change, or (iii) degradation of most FBPs is repressed upon MLN4924 treatment. The first explanation seems unlikely because it would require a complex mechanism to coordinate the simultaneous up-regulation of many FBPs. The second explanation is intriguing, but as of yet there is no evidence to support or discount it. The third explanation is consistent with what is currently known about FBP autoregulation. Many FBPs have been shown to be unstable, and degradation is often (34, 35), but not always (36, 37), dependent on SCF activity, suggesting that auto-ubiquitination of FBPs within SCF complexes underlies their turnover. Blockade of SCF activity with MLN4924 would be predicted to suppress auto-ubiquitination-dependent turnover of FBPs. It remains unclear why the deneddylated SCF complexes that accumulated in MLN4924-treated cells were not disassembled by Cand1, given that Cand1 can displace FBP-Skp1 from unmodified Cul1 *in vitro* (16, 17). It is possible that Cand1 does not possess this activity *in vivo*, or that Cand1 does displace FBP-Skp1 modules from unmodified Cul1, but that the reaction is freely reversible such that the overall equilibrium between Cand1, Cul1, and FBP-Skp1 does not change. Future experiments should aim to distinguish between these various possibilities.

In summary, we have investigated the Cul1 proteome using high accuracy mass spectrometry. We found common shared subunits Skp1 and Rbx1, regulators such as CSN, Dcund1, 2, 4, and 5 and Cand1 and 2, as well as 42 different FBPs associated with Cul1. These F-box proteins exhibited substantial differences in their abundance, and most of the abundant F-box proteins remain to be characterized. Using a quantitative SILAC approach, we observed, contrary to expectation, that deneddylation leads to a net increase in SCF complexes. Our results suggest that current models of the Cul1 cycle do not adequately capture the mechanisms that sculpt the repertoire of SCF complexes *in vivo*. Future work will aim to understand how Nedd8 deconjugation, FBP dissociation, and FBP turnover cooperate to control the Cul1 cycle in cells.

Acknowledgments—We thank P. Kaiser for the HTBH tag and J. Wade Harper for generously sharing results prior to publication. MLN4924 was a generous gift from Millennium: The Takeda Oncology Company.

* J. E. Lee was supported by the Ruth L. Kirschstein NRSA fellowship (CA138126) and the Proteome Exploration lab was supported by the Beckman Institute at Caltech and an award from the Gordon and Betty Moore Foundation. R. J. D. is an Investigator of the Howard Hughes Medical Institute and this work was supported in part by HHMI and an NIH grant (GM065997) to R. J. D.

S This article contains supplemental Table 1–2.

‖ To whom correspondence should be addressed: Division of Biology, California Institute of Technology, 1200 E California Blvd M/C 156-29, Pasadena, CA 91125, e-mail: deshaies@caltech.edu.

REFERENCES

1. Pickart, C. M. (2001) Mechanisms underlying ubiquitination. *Ann. Rev. Biochem.* **70,** 503–533
2. Chau, V., Tobias, J. W., Bachmair, A., Marriott, D., Ecker, D. J., Gonda, D. K., and Varshavsky, A. (1989) A multiubiquitin chain is confined to specific lysine in a targeted short-lived protein. *Science* **243,** 1576–1583
3. Pierce, N. W., Kleiger, G., Shan, S. O., and Deshaies, R. J. (2009) Detection of sequential polyubiquitylation on a millisecond timescale. *Nature* **462,** 615–619
4. Soucy, T. A., Smith, P. G., Milhollen, M. A., Berger, A. J., Gavin, J. M., Adhikari, S., Brownell, J. E., Burke, K. E., Cardin, D. P., Critchley, S., Cullis, C. A., Doucette, A., Garnsey, J. J., Gaulin, J. L., Gershman, R. E., Lublinsky, A. R., McDonald, A., Mizutani, H., Narayanan, U., Olhava, E. J., Peluso, S., Rezaei, M., Sintchak, M. D., Talreja, T., Thomas, M. P., Traore, T., Vyskocil, S., Weatherhead, G. S., Yu, J., Zhang, J., Dick, L. R., Claiborne, C. F., Rolfe, M., Bolen, J. B., and Langston, S. P. (2009) An inhibitor of NEDD8-activating enzyme as a new approach to treat cancer. *Nature* **458,** 732–736
5. Petroski, M. D., and Deshaies, R. J. (2005) Function and regulation of cullin-RING ubiquitin ligases. *Nat. Rev. Mol. Cell Biol.* **6,** 9–20
6. Jin, J., Cardozo, T., Lovering, R. C., Elledge, S. J., Pagano, M., and Harper, J. W. (2004) Systematic analysis and nomenclature of mammalian F-box proteins. *Genes Dev.* **18,** 2573–2580
7. Kaplan, K. B., Hyman, A. A., and Sorger, P. K. (1997) Regulating the yeast kinetochore by ubiquitin-dependent degradation and Skp1p-mediated phosphorylation. *Cell* **91,** 491–500
8. Galan, J. M., Wiederkehr, A., Seol, J. H., Haguenauer-Tsapis, R., Deshaies, R. J., Riezman, H., and Peter, M. (2001) Skp1p and the F-box protein Rcy1p form a non-SCF complex involved in recycling of the SNARE Snc1p in yeast. *Mol. Cell. Biol.* **21,** 3105–3117
9. Cope, G. A., and Deshaies, R. J. (2003) COP9 signalosome: a multifunctional regulator of SCF and other cullin-based ubiquitin ligases. *Cell* **114,** 663–671
10. Schmidt, M. W., McQuary, P. R., Wee, S., Hofmann, K., and Wolf, D. A. (2009) F-box-directed CRL complex assembly and regulation by the CSN and CAND1. *Mol. Cell* **35,** 586–597
11. Bosu, D. R., and Kipreos, E. T. (2008) Cullin-RING ubiquitin ligases: global regulation and activation cycles. *Cell Div.* **3,** 7
12. Duda, D. M., Borg, L. A., Scott, D. C., Hunt, H. W., Hammel, M., and Schulman, B. A. (2008) Structural insights into NEDD8 activation of cullin-RING ligases: conformational control of conjugation. *Cell* **134,** 995–1006
13. Saha, A., and Deshaies, R. J. (2008) Multimodal activation of the ubiquitin ligase SCF by Nedd8 conjugation. *Mol. Cell* **32,** 21–31
14. Yamoah, K., Oashi, T., Sarikas, A., Gazdoiu, S., Osman, R., and Pan, Z. Q. (2008) Autoinhibitory regulation of SCF-mediated ubiquitination by human cullin 1's C-terminal tail. *Proc. Natl. Acad. Sci. U.S.A.* **105,** 12230–12235
15. Lyapina, S., Cope, G., Shevchenko, A., Serino, G., Tsuge, T., Zhou, C., Wolf, D. A., Wei, N., Shevchenko, A., and Deshaies, R. J. (2001) Promotion of NEDD-CUL1 conjugate cleavage by COP9 signalosome. *Science* **292,** 1382–1385
16. Goldenberg, S. J., Cascio, T. C., Shumway, S. D., Garbutt, K. C., Liu, J., Xiong, Y., and Zheng, N. (2004) Structure of the Cand1-Cul1-Roc1 complex reveals regulatory mechanisms for the assembly of the multisubunit cullin-dependent ubiquitin ligases. *Cell* **119,** 517–528
17. Zheng, J., Yang, X., Harrell, J. M., Ryzhikov, S., Shim, E. H., Lykke-Andersen, K., Wei, N., Sun, H., Kobayashi, R., and Zhang, H. (2002) CAND1 binds to unneddylated CUL1 and regulates the formation of SCF ubiquitin E3 ligase complex. *Mol. Cell* **10,** 1519–1526
18. Bornstein, G., Bloom, J., Sitry-Shevah, D., Nakayama, K., Pagano, M., and Hershko, A. (2003) Role of the SCFSkp2 ubiquitin ligase in the degradation of p21Cip1 in S phase. *J. Biol. Chem.* **278,** 25752–25757
19. Liu, J., Furukawa, M., Matsumoto, T., and Xiong, Y. (2002) NEDD8 modification of CUL1 dissociates p120(CAND1), an inhibitor of CUL1-SKP1 binding and SCF ligases. *Mol. Cell* **10,** 1511–1518
20. Tagwerker, C., Flick, K., Cui, M., Guerrero, C., Dou, Y., Auer, B., Baldi, P.,

Huang, L., and Kaiser, P. (2006) A tandem affinity tag for two-step purification under fully denaturing conditions: application in ubiquitin profiling and protein complex identification combined with in vivocross-linking. *Mol. Cell Proteomics* **5,** 737–748
21. Cronan, J. E., Jr. (1990) Biotination of proteins in vivo. A post-translational modification to label, purify, and study proteins. *J. Biol. Chem.* **265,** 10327–10333
22. Hess, S., van Beek, J., and Pannell, L. K. (2002) Acid hydrolysis of silk fibroins and determination of the enrichment of isotopically labeled amino acids using precolumn derivatization and high-performance liquid chromatography-electrospray ionization-mass spectrometry. *Anal. Biochem.* **311,** 19–26
23. de, Godoy, L. M., Olsen, J. V., Cox, J., Nielsen, M. L., Hubner, N. C., Fröhlich, F., Walther, T. C., and Mann, M. (2008) Comprehensive mass-spectrometry-based proteome quantification of haploid versus diploid yeast. *Nature* **455,** 1251–1254
24. Cox, J., and Mann, M. (2008) MaxQuant enables high peptide identification rates, individualized p.p.b.-range mass accuracies and proteome-wide protein quantification. *Nat. Biotechnol.* **26,** 1367–1372
25. Finn, R. D., Mistry, J., Tate, J., Coggill, P., Heger, A., Pollington, J. E., Gavin, O. L., Gunasekaran, P., Ceric, G., Forslund, K., Holm, L., Sonnhammer, E. L., Eddy, S. R., and Bateman, A. (2010) The Pfam protein families database. *Nucleic Acids Res.* **38,** D211–222
26. Ishihama, Y., Oda, Y., Tabata, T., Sato, T., Nagasu, T., Rappsilber, J., and Mann, M. (2005) Exponentially modified protein abundance index (emPAI) for estimation of absolute protein amount in proteomics by the number of sequenced peptides per protein. *Mol. Cell Proteomics* **4,** 1265–1272
27. Zheng, N., Schulman, B. A., Song, L., Miller, J. J., Jeffrey, P. D., Wang, P., Chu, C., Koepp, D. M., Elledge, S. J., Pagano, M., Conaway, R. C., Conaway, J. W., Harper, J. W., and Pavletich, N. P. (2002) Structure of the Cul1-Rbx1-Skp1-F boxSkp2 SCF ubiquitin ligase complex. *Nature* **416,** 703–709
28. Brownell, J. E., Sintchak, M. D., Gavin, J. M., Liao, H., Bruzzese, F. J., Bump, N. J., Soucy, T. A., Milhollen, M. A., Yang, X., Burkhardt, A. L., Ma, J., Loke, H. K., Lingaraj, T., Wu, D., Hamman, K. B., Spelman, J. J., Cullis, C. A., Langston, S. P., Vyskocil, S., Sells, T. B., Mallender, W. D., Visiers, I., Li, P., Claiborne, C. F., Rolfe, M., Bolen, J. B., and Dick, L. R. (2010) Substrate-assisted inhibition of ubiquitin-like protein-activating enzymes: the NEDD8 E1 inhibitor MLN4924 forms a NEDD8-AMP mimetic in situ. *Mol. Cell* **37,** 102–111
29. Kleiger, G., Saha, A., Lewis, S., Kuhlman, B., and Deshaies, R. J. (2009) Rapid E2-E3 assembly and disassembly enable processive ubiquitylation of cullin-RING ubiquitin ligase substrates. *Cell* **139,** 957–968
30. Wolf, D. A., McKeon, F., and Jackson, P. K. (1999) F-box/WD-repeat proteins pop1p and Sud1p/Pop2p form complexes that bind and direct the proteolysis of cdc18p. *Curr. Biol.* **9,** 373–376
31. Kominami, K., Ochotorena, I., and Toda, T. (1998) Two F-box/WD-repeat proteins Pop1 and Pop2 form hetero- and homo-complexes together with cullin-1 in the fission yeast SCF (Skp1-Cullin-1-F-box) ubiquitin ligase. *Genes Cells* **3,** 721–735
32. Lisztwan, J., Marti, A., Sutterlüty, H., Gstaiger, M., Wirbelauer, C., and Krek, W. (1998) Association of human CUL-1 and ubiquitin-conjugating enzyme CDC34 with the F-box protein p45(SKP2): evidence for evolutionary conservation in the subunit composition of the CDC34-SCF pathway. *EMBO J.* **17,** 368–383
33. Hwang, J. W., Min, K. W., Tamura, T. A., and Yoon, J. B. (2003) TIP120A associates with unneddylated cullin 1 and regulates its neddylation. *FEBS Lett.* **541,** 102–108
34. Zhou, P., and Howley, P. M. (1998) Ubiquitination and degradation of the substrate recognition subunits of SCF ubiquitin-protein ligases. *Mol. Cell* **2,** 571–580
35. Galan, J. M., and Peter, M. (1999) Ubiquitin-dependent degradation of multiple F-box proteins by an autocatalytic mechanism. *Proc. Natl. Acad. Sci. U.S.A.* **96,** 9124–9129
36. Wei, W., Ayad, N. G., Wan, Y., Zhang, G. J., Kirschner, M. W., and Kaelin, W. G., Jr. (2004) Degradation of the SCF component Skp2 in cell-cycle phase G1 by the anaphase-promoting complex. *Nature* **428,** 194–198
37. Bashir, T., Dorrello, N. V., Amador, V., Guardavaccaro, D., and Pagano, M. (2004) Control of the SCF(Skp2-Cks1) ubiquitin ligase by the APC/C(Cdh1) ubiquitin ligase. *Nature* **428,** 190–193